
Mathematical modeling of hydromagnetic squeeze film in longitudinally rough conducting truncated conical plates considering slip velocity

Dr. Jatin V. Adeshara¹, Dr. Hardik P. Patel², Suresh G. Sorathiya³,

Dr. Gunamani B. Deheri⁴, Rakesh M. Patel⁵

1. Assistant Professor, Vishwakarma Government Engineering College, Chandkheda, Ahmedabad – 382424.
2. Department of Humanity and Science, LJIET, L J K University, Ahmedabad.
3. Associate Professor, Department of Mathematics, Shreyarth University, Ahmedabad. Email: drsuresh.sorathiya@gmail.com
4. Department of Mathematics, S. P. University, VallabhVidyanagar – 388 120.
5. Department of Mathematics, Gujarat Arts and Science College, Ahmedabad – 380 006.

Abstract:

In an effort to analyze the behavior of a hydromagnetic fluid-based squeeze film (S.F.) between rough truncated conical plates (T.C.P.), the consequences of slip velocity have been taken into consideration. The influence of slip velocity has been incorporated into Beavers and Joseph's theory. Use a different kind of probability density function (P.D.F.), It has been decided to use the Christensen & Tonder (C&T) model to assess the impact of longitudinal surface roughness (L.R.) and the stochastically averaged. The expression for pressure distribution (P.D) has been derived by solving the Reynolds' type equation. As a result, the load carrying capacity (L.C.C.) is calculated. The graphical representations clearly show that despite the effect of slip velocity is relatively unfavorable, the magnetic fluid (M.F.) lubricant only partially improves the situation, at least when it comes to the roughness that is negatively skewed. The slip parameter should be reduced to improve the bearing system's performance overall. When variance (negative) is present, an appropriate aspect ratio and semi-vertical angle may result in some mitigation for the detrimental effect of slip velocity.

Keywords:

Slip velocity, Truncated Conical plates, longitudinal roughness, load bearing capacity, conductivity.

Introduction:

The squeeze films (S.F.) among spongy plates of several forms, such as circular, annular, were examined by Prakash & Vij [1]. With all other parameters staying the same, this experiment compared the S.F. performances of different geometries of comparable surface area, and it was found that circular plates had the maximum transient L.B.C. Numerous studies [Verma [2]; Bhat & Deheri [3-4]] have investigated and used M.F. as a lubricant to alter the performance of a bearing system. This study proved that increasing the magnetization enhanced the L.B.C. When compared to annular plates, the S.F. performance in circular disks had greatly improved. The combined impact of couple stresses and irregularity was researched by Hsiu et al [5]. The attitude angle and friction parameters decreased as a result of the transverse roughness (T.R.), while the impact of L.R. remained almost the opposite of that of the T.R. In order to study the impact of surface irregularity on the performance of a M.F.-based S.F. between rough, spongy, T.C.P, Deheri et al [6] expanded the research of Bhat & Deheri [4]. The (C. & T.) [7-9] stochastic model was used in this experiment to assess the impact of T.R. According to Deheri et al.'s analysis [6], there may be a chance for the magnetization to reduce the harmful effects of irregularity, at least in the case of negatively skewed irregularity.

The performance of a S.F. in spherical bearing was examined by Gupta & Deheri [10] in relation to the impact of T.R. It was discovered that of the three irregularity factors, skewness had the greatest impact on the system and produced a reduction in load. In their discussion of the impact of T.R. on a hydrodynamic slider bearing's performance using a stochastic model, Andharia et al. [11] discovered that T.R. generally had a negative impact. However, when (-) variance was present, the situation remained significantly better, and this favorable impact was facilitated by the negative skewed irregularity. It was demonstrated that surface irregularity generally had a negative impact. When comparatively larger quantities of standard deviation (S.D.) were involved, the spinning inertia made the problem much worse. Here, it was determined that minimizing the deformation impact was necessary to offset the negative effects of porosity and S.D. with the benefits of magnetization.

Analysis:

Two T.C.P structure the bearing system. The top plate advances toward the bottom plate. The backing is solid and the bearing surfaces are L.R.

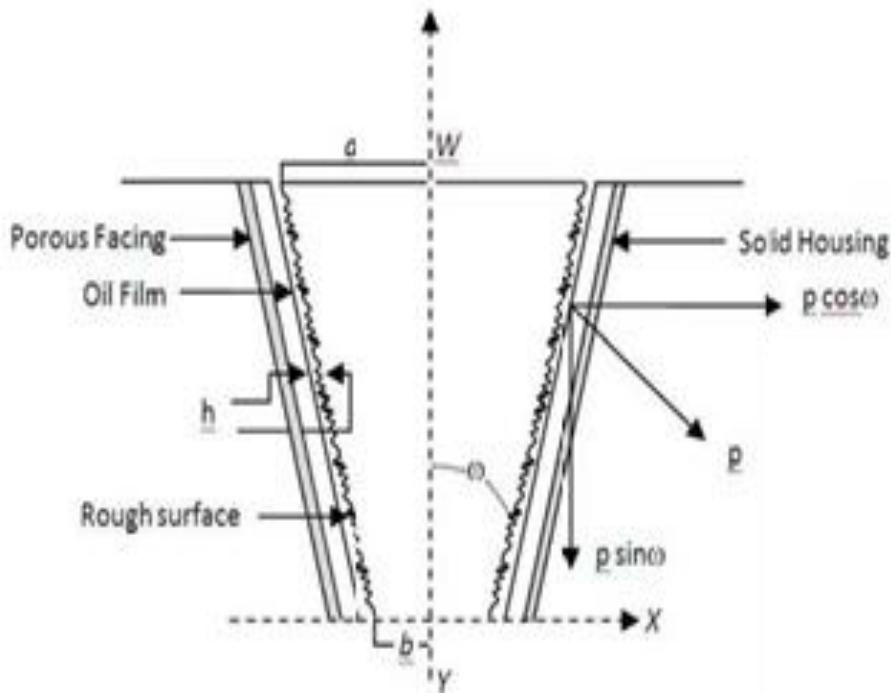


Fig. 1. Configuration of truncated conical plates

The clearance gap between the plates is filled with an electrically conducting lubricant since the plates are thought to be electrically conductive. Transverse magnetic field applied uniformly between the plates. The bearing surfaces are presumably L.R.

$$x^{-1} \frac{d}{dx} \left(x \frac{dp}{dx} \right) = \frac{A \mu h}{\left[\frac{2}{M^3} \left(\tanh \frac{M}{2} - \frac{M}{2} \right) \right]} \cdot \frac{1}{\left[\frac{1 + \phi_1 + \phi_0}{\frac{\tanh(M/2)}{1} * \left(\frac{2}{M} \right)^{-1} + (\phi_1 + \phi_0)} \right]}$$

(1)

where

$$A = h^{-3} [1 - ah^{-1} + 6h^{-2}(\sigma^2 + \alpha^2) - 10h^{-3}(\epsilon + 3\sigma^2\alpha + \alpha^3)] (1+4s)/(1+2s)$$

Application of B.C. to the solution of this equation

$$P(\operatorname{acosec} \omega) = 0;$$

$$p(\operatorname{bcosec} \omega) = 0$$

(2)

Establishes the P.D.

$$p = \frac{-h \left(a^2 - b^2 \right) \cos ec^2 \omega \cdot \left[\frac{\ln(x/\operatorname{bcosec} \omega)}{\ln(a/b)} - \frac{(x \sin \omega/b)^2 - 1}{(a/b)^2 - 1} \right] A}{4 \left[\frac{2}{M^3} \left(\tanh \frac{M}{2} - \frac{M}{2} \right) \right]} \cdot \left[\frac{1}{\frac{1 + \phi_1 + \phi_0}{\frac{\tanh(M/2)}{1} * \left(\frac{2}{M} \right)^{-1} + (\phi_0 + \phi_1)}} \right]$$

Here

$$A = h^{-3} [1 - \alpha h^{-1} + 6h^{-2}(\sigma^2 + \alpha^2) - 10h^{-3}(\epsilon + 3\sigma^2\alpha + \alpha^3)] \bullet (1 + 4s)/(1 + 2s)$$

It is possible to derive the non-dimensional pressure distribution.

$$P = \frac{-ph^3}{\pi * \mu * h^3 * \left(a^2 - b^2 \right) \cos ec \omega} = \frac{\cos ec \omega \cdot \left[\frac{\ln(x \sin \omega/b)}{\ln(a/b)} - \frac{(x \sin \omega/b)^2 - 1}{(a/b)^2 - 1} \right] B}{4 * \pi \left[\frac{2}{M^3} \left(\tanh \frac{M}{2} - \frac{M}{2} \right) \right]} \cdot \left[\frac{1}{\frac{1 + \phi_1 + \phi_0}{\frac{\tanh(M/2)}{1} * \left(\frac{2}{M} \right)^{-1} + (\phi_1 + \phi_0)}} \right] \tag{3}$$

Where in

$$B = \left[1 + \alpha^*^3 - 3\alpha^* - 10(\epsilon^* + 3\sigma^*^2 \alpha^* + 6(\sigma^*^2 + \alpha^*^2)) \right] \bullet (1 + 4s^*)/(1 + 2s^*)$$

Where

$$\sigma^* = \frac{\sigma}{h}, \alpha^* = \frac{\alpha}{h}, \epsilon^* = \frac{\epsilon}{h^3}$$

Then the L.B.C. given by

$$w = 2 * \pi \int_{b \operatorname{cosec} \omega}^{a \operatorname{cosec} \omega} p \cdot x dx$$

As is represented in dimensional as

$$w = \frac{-h \pi (a^2 - b^2) \operatorname{cosec}^4 \omega \cdot \left[(a^2 + b^2) - \frac{(a^2 - b^2)}{\ln(a/b)} \right] B}{8 * \left[\frac{2}{M^3} \left(\tanh \frac{M}{2} - \frac{M}{2} \right) \right]} \cdot \left[\frac{1}{\phi_1 + \phi_0 + \frac{\tanh(M/2)}{1} * \left(\frac{2}{M} \right)^{-1}} \right]$$

The L.B.C. is obtained as dimensionless

$$W = - \frac{wh^3}{\mu h^2 (a^2 - b^2)^2 \operatorname{cosec}^2 \omega} \operatorname{cosec}^2 \omega \cdot \left[\frac{(a/b)^2 + 1}{(a/b)^2 - 1} - \frac{1}{\ln(a/b)} \right] B$$

$$= \frac{1}{8 * \pi \left[\frac{2}{M^3} \left(\tanh \frac{M}{2} - \frac{M}{2} \right) \right]} \cdot \left[\frac{1}{\phi_1 + \phi_0 + \frac{\tanh(M/2)}{1} * \left(\frac{2}{M} \right)^{-1}} \right]$$

(4)

Results and discussions

Equation (3) clearly determines the P.D., whereas equation (4) provides the formula for the L.B.C. These performance traits are influenced by a variety of factors, including M, $\phi_0 + \phi_1$, $\sigma^*, \alpha^*, \varepsilon^*, k, s^*$ and \square . The effects of the cone's M, $\phi_0 + \phi_1$, $\sigma^*, \alpha^*, \varepsilon^*, k, s^*$ and \square are all described by these characteristics, in that order. By lowering the irregularity parameters, M, and $\phi_0 + \phi_1$ to zero, this study decreases the observation of Prakash & Vij [1]. Finally, this work results in the contributions of Dodge et al (1965), and Sinha & Gupta (1974) under certain circumstances, assuming the irregularity parameters to be zero.

Results and Discussion:

For given values $M, \sigma^*, \alpha^*, \varepsilon^*, k, s^*$ and \square . It is obvious that the L.B.C. improves as the $\phi_0 + \phi_1$ increases. Additionally, the factor is how conductivity affects the pressure distribution P.D. and L.B.C.

$$\left(\frac{\phi_1 + \phi_0 + \frac{\tanh(M/2)}{1} * \left(\frac{2}{M}\right)^{-1}}{\phi_1 + \phi_0 + 1} \right)$$

This tends to $\frac{\phi_1 + \phi_0}{\phi_1 + \phi_0 + 1}$ as $\tanh M \sim 1, 2/M \sim 0$ for large values of M . It is clear that

these two functions increase the functionality of $\phi_1 + \phi_0$. Additionally, it can be seen from mathematical analysis that the carrying capacity of pressure and load grows as $\phi_0 + \phi_1$ somewhere else. It's important to keep in mind that even in the absence of flow, the bearing with magnetic field can support a load.

Figures (1–7) depict the variation in the L.B.C in relation to the M for various values of the $\phi_0 + \phi_1, \sigma^*, \alpha^*, \varepsilon^*, k, s^*$, and \square , respectively. These numbers clearly show that the L.B.C. grows significantly with regard to the M where the influence of (-ve) all α^* is most pronounced, followed by ω . Furthermore, the increase in L.B.C. for the M and $\square \square \square$ combination is comparatively low compared to the other situations, and the initial effect of the σ^* is very negligible. The σ^* impact is also quite detrimental. The distribution of L.B.C. with regard to $\phi_0 + \phi_1$ for various parameter values $\alpha^*, s^*, \sigma^*, k, \varepsilon^*$, and ω is shown in Figures (8-13). It has been discovered that $\phi_0 + \phi_1$ tends to enhance L.B.C., and the rate of growth in the beginning is substantially higher. In this case, the combined impact of k and $\phi_0 + \phi_1$ is considerably superior to the combined effect of $\phi_0 + \phi_1, (-)\varepsilon^*$ and $\phi_0 + \phi_1$ together have a significantly higher effect than $(-)\alpha^*$ and $\phi_0 + \phi_1$ together. Additionally, it should be emphasized that, in terms of the increase in L.B.C. the combined effect of $\phi_0 + \phi_1$ and k falls somewhere between the effects of negative α^* and ε^* .

The L.B.C. distribution profile for the σ^* associated with irregularity is shown in Figures (14–18) for various values of $\alpha^*, \varepsilon^*, k, s^*$, and \square . In the event of ε^* , the rate of

reduction is more pronounced. Figures (19-22) show the variation in L.B.C. with regard to α^* for various values of ε^* , k , s^* , and \square . While α^* (+ve) enhances the L.B.C., the (-ve) α^* also increases it, but at more quickly when the k is taken into account. Figures (23-25) demonstrate that negatively skewed irregularity increases load in a manner similar to how α^* (ve) does. For positively skewed irregularity and α^* (+ve), these tendencies are reversed. Figure (26), which shows the influence of k and ω , demonstrates that the effect of k is clearly positive and that the L.B.C. rises with higher values of the k . It is interesting to notice that the influence on L.B.C. rises when the (k) aspect ratio is more than k in comparison to the ω , as shown in Figure (26-27), As shown in figure (28), the influence of slip velocity on the distribution of L.B.C. grows at increasing values of the s^* .

Conclusion:

This analysis clearly shows that while developing the bearing system, the irregularity issues must be given attention. The slip parameter must be kept to a minimum for the bearing to operate well overall. Most likely, even when a greater value of the slip parameter is involved, the increased viscosity caused by magnetization keeps the load bearing capacity from declining. Even in the case of negatively skewed roughness and negative variance, there is, of course, a limited effect of magnetization in these kinds of systems since the load bearing capacity is drastically reduced due to the negative effects of standard deviation, porosity, deformation, and slip velocity.

References:

1. Prakash, J. & Vij, S. K. (1973). Load capacity and time height relation between spongy plates. *Wear*, Vol. 24, pp. 309-322.
2. Verma, P. D. S. (1986). Magnetic fluid-based squeeze film. *International Journal of Engineering Science*, Vol. 24, No. 3, pp. 305-401.
3. Bhat, M. V. & Deheri, G. M. (1991). Squeeze film behavior in spongy annular disks lubricated with magnetic fluid. *Wear*, Vol.151, pp. 123-128.
4. Bhat, M. V. & Deheri, G. M. (1992). Magnetic fluid based squeeze film between two curved circular plates. *Bulletin of Calcutta Mathematical Society*, Vol. 85, pp. 521-524.

5. Hsiu , Chiang, Lu., Cheng, Hsu, H. & Lin, J. R. (2004), Lubrication performance of long journal bearings considering effects of couple stresses and surface roughness. Journal of the Chinese Institute of Engineers, Vol.27, No. 2, pp. 287-292.
6. Deheri, G. M., Patel, H. C. & Patel, R. M. (2007). Magnetic fluid-based squeeze film between rough spongy truncated conical plates. Journal of Engineering Tribology, Vol. 221, Part J, pp. 515- 523.
7. Christensen, H. & Tonder, K. C. (1969a). Tribology of rough surfaces: stochastic models of hydrodynamic lubrication. SINTEF Report No.10/69-18.
8. Christensen, H. & Tonder, K. C. (1969b). Tribology of rough surfaces: parametric study and comparison of lubrication model. SINTEF Report No.22/69-18.
9. Christensen, H. & Tonder, K. C. (1970). The hydrodynamic lubrication of rough bearing surfaces of finite width. ASME-ASLE Lubrication Conference, Paper no.70-lub-7.
10. Gupta, J. L. & Deheri, G. M. (1996), Effect of roughness on the behavior of squeeze film in a spherical bearing. Tribology Transaction, Vol. 39, pp. 99-102.
11. Andharia, P. I., Gupta, J. L. & Deheri, G. M. (2001), Effects of surface roughness and hydrodynamic lubrications of slider bearings, Tribology Transaction, Vol. 44, No. 2, pp. 291-297.

Numerical Values

M	4	6	8	10	12
$\phi_0 + \phi_1$	0	1	2	3	4
σ^*	0	0.05	0.1	0.15	0.2
α^*	-0.05	-0.03	0	0.03	0.05
ε^*	-0.05	-0.03	0	0.03	0.05
k	1.5	1.75	2.0	2.25	2.5
s^*	0.1	0.2	0.3	0.4	0.5
\square	30	40	50	60	7

Figure: 1 load of M & $\phi_0 + \phi_1$

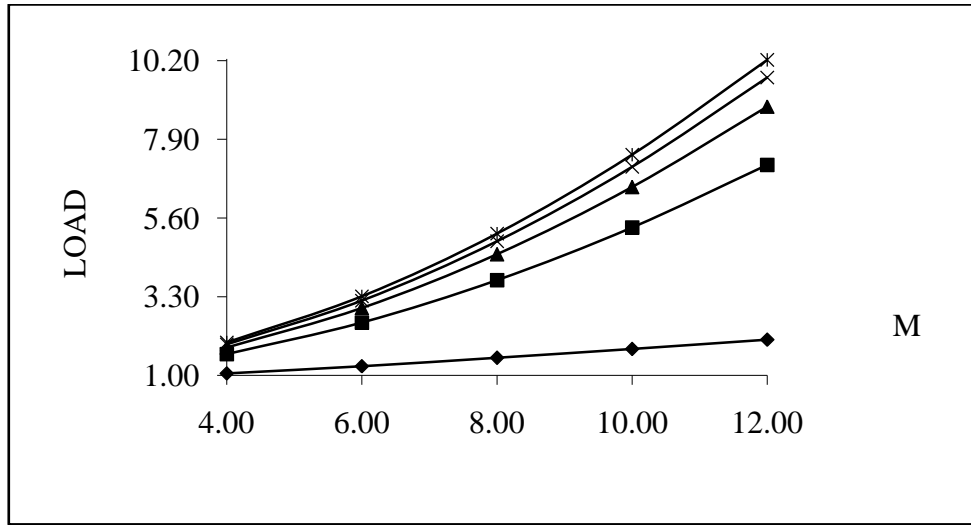


Figure: 2 load of M & σ^*

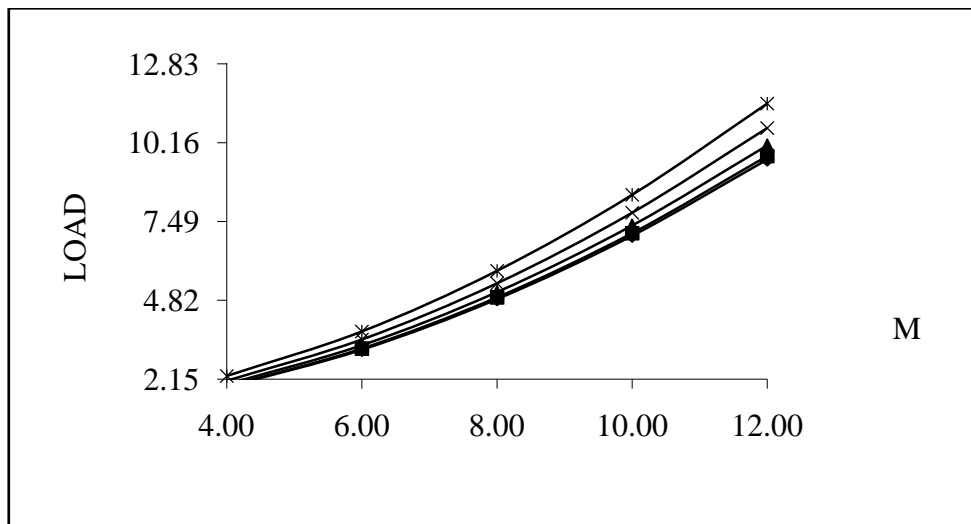


Figure: 3 load of M & α^*

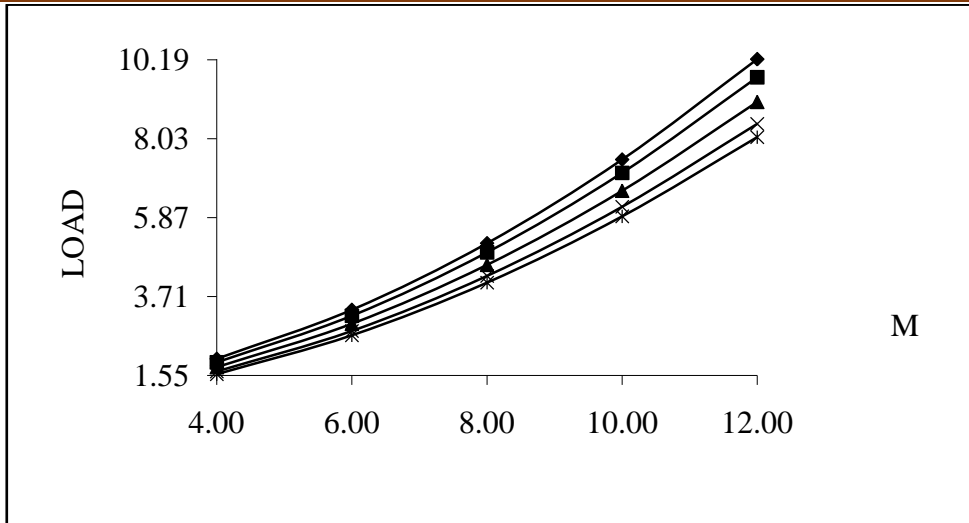


Figure: 4 load of M & ϵ^*

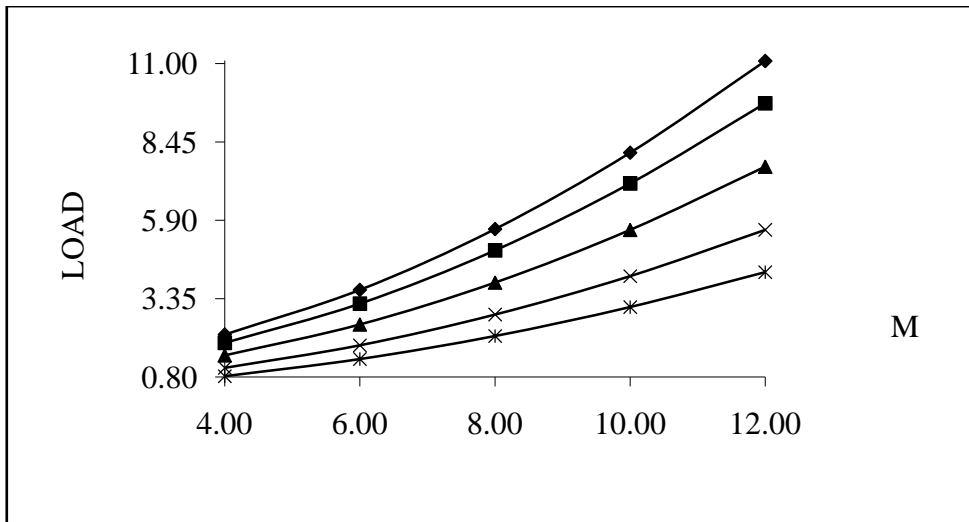


Figure: 5 load of M & k

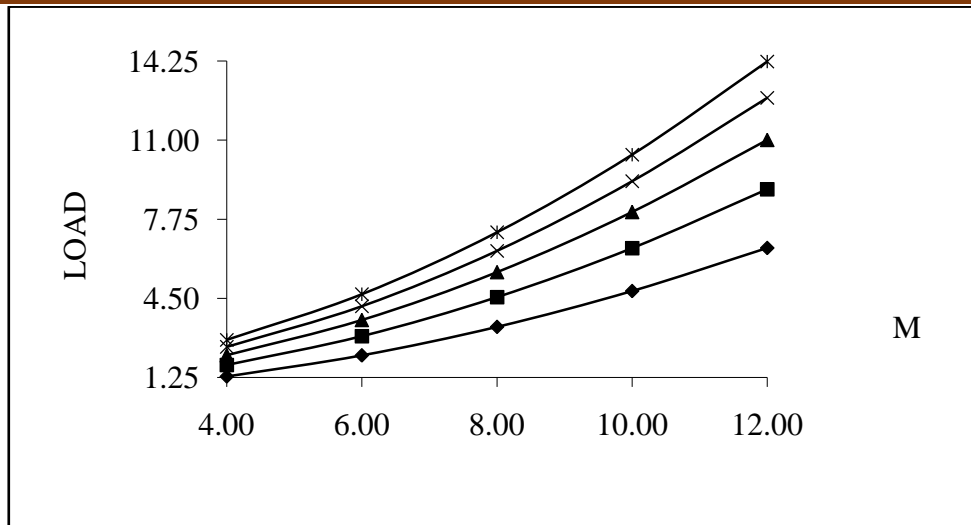


Figure: 6 load of M & □

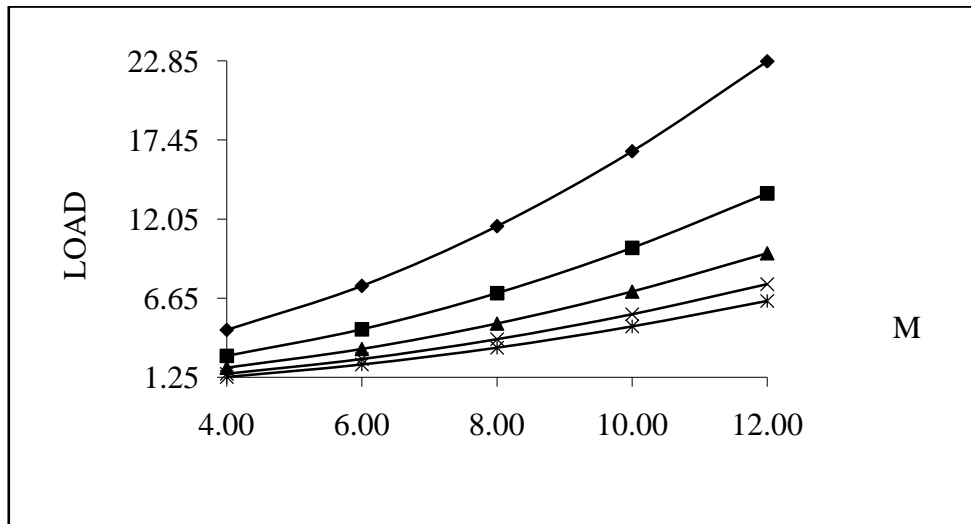


Figure: 7 load of M & s*

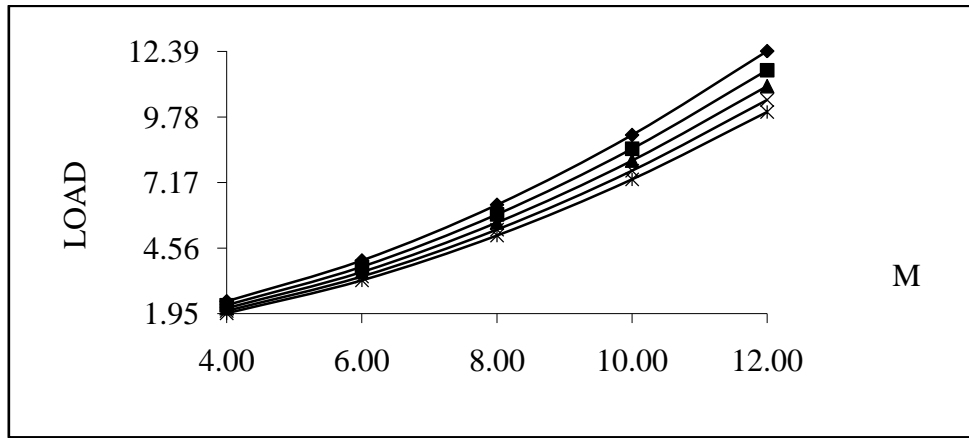


Figure: 8 load of $\phi_0 + \phi_1$ & σ^*

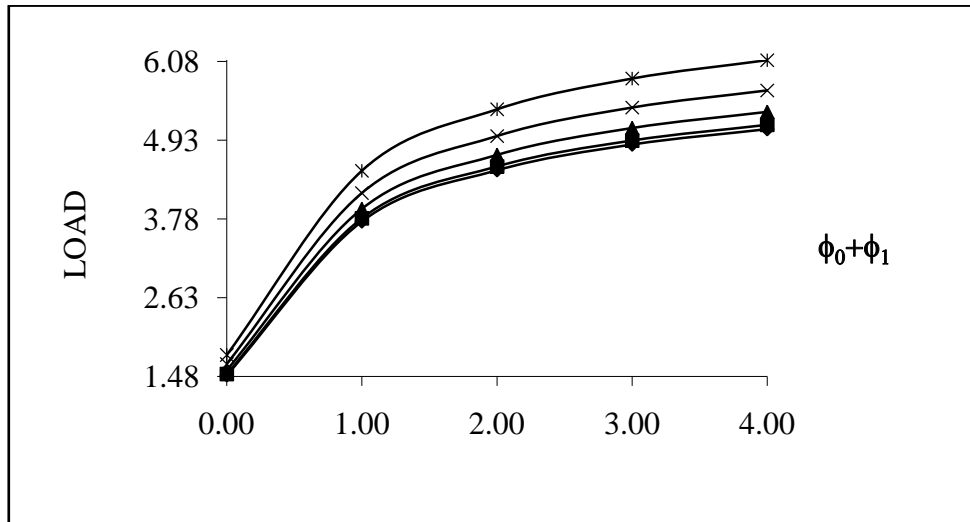


Figure: 9 load of $\phi_0 + \phi_1$ & α^*

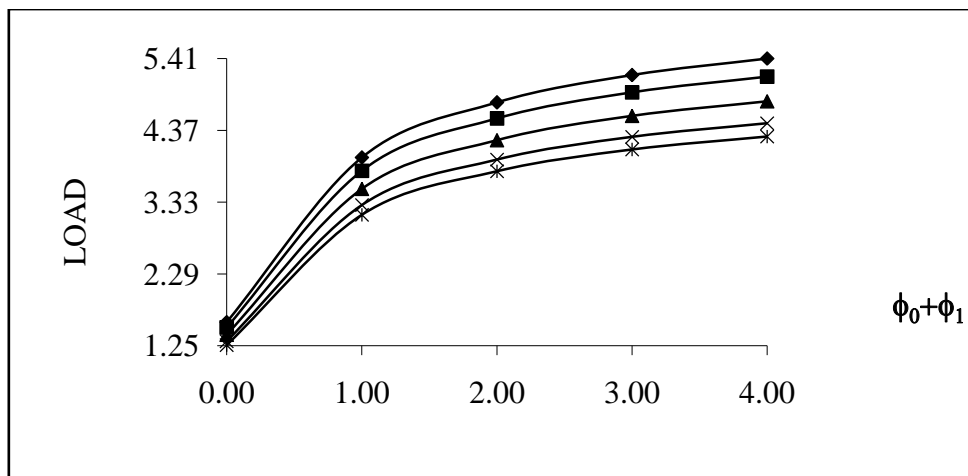


Figure: 10 load of $\phi_0 + \phi_1$ & ε^*

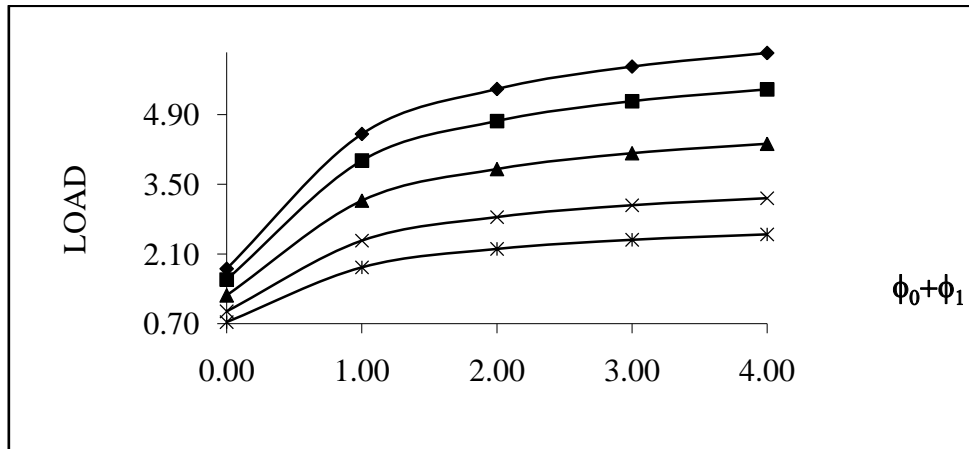


Figure: 11 load of $\phi_0 + \phi_1$ & k

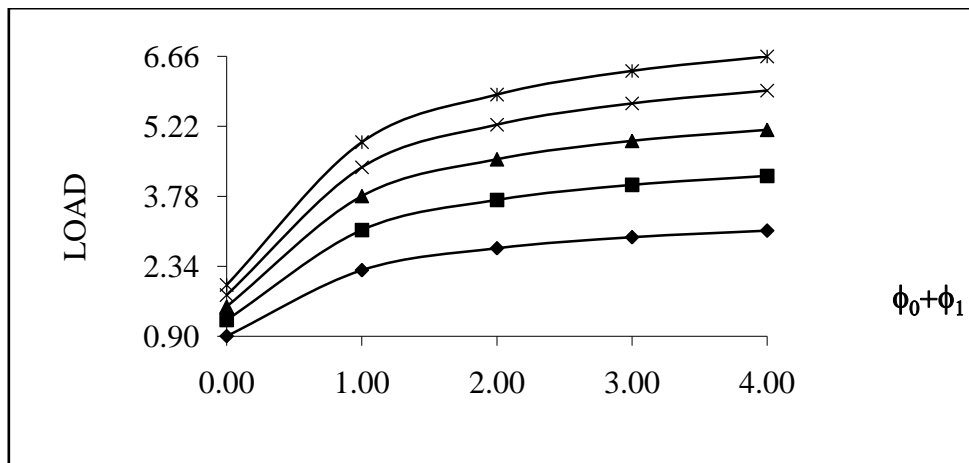


Figure: 12 load of $\phi_0 + \phi_1$ and \square

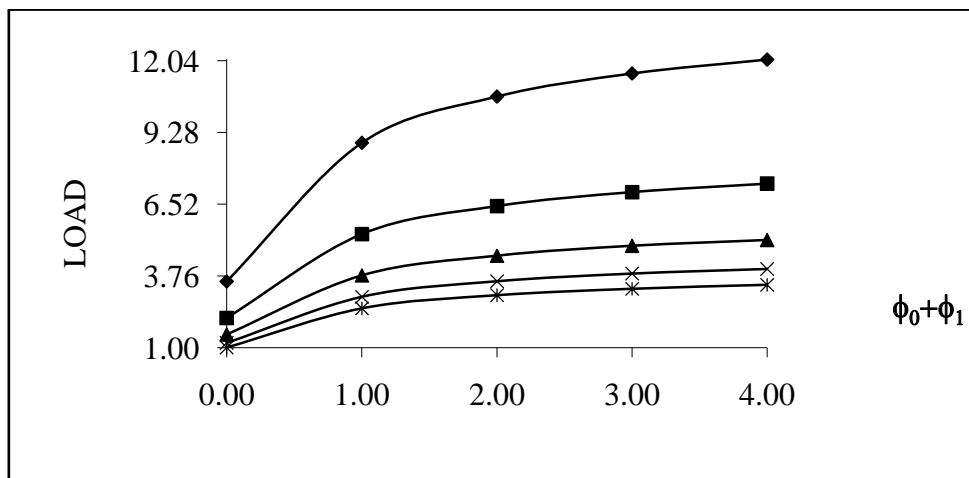


Figure: 13 load of $\phi_0 + \phi_1$ & s^*

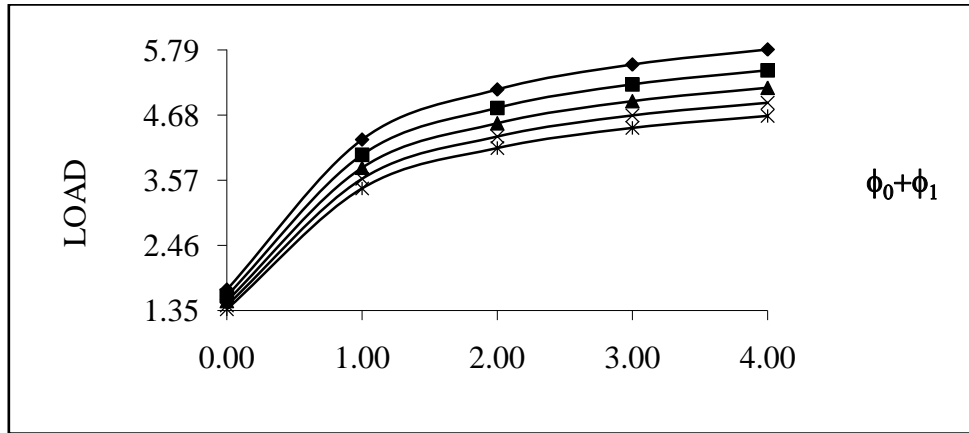


Figure: 14 load of σ^* & α^*

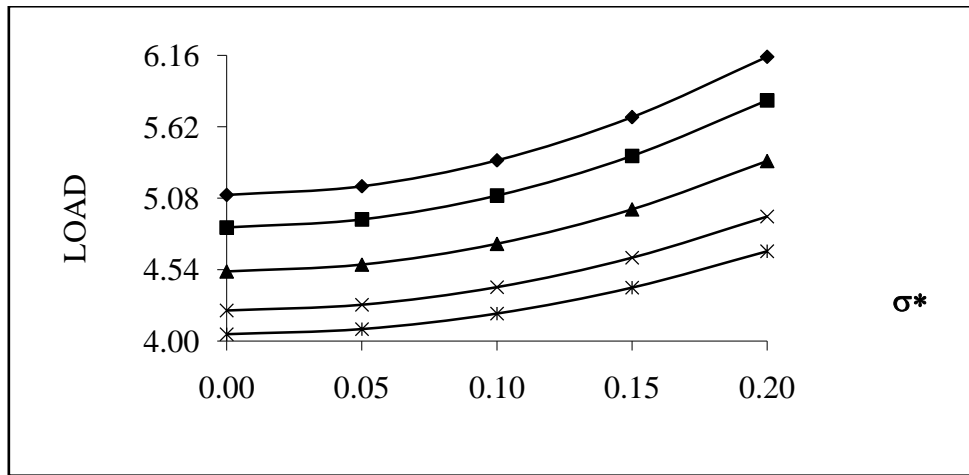


Figure: 15 load of σ^* & ϵ^*

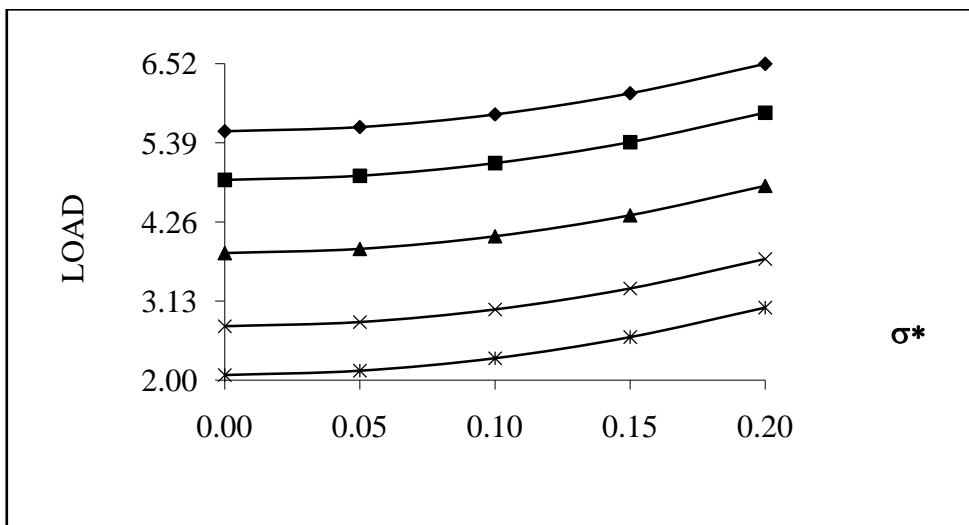


Figure: 16 load of σ^* & k

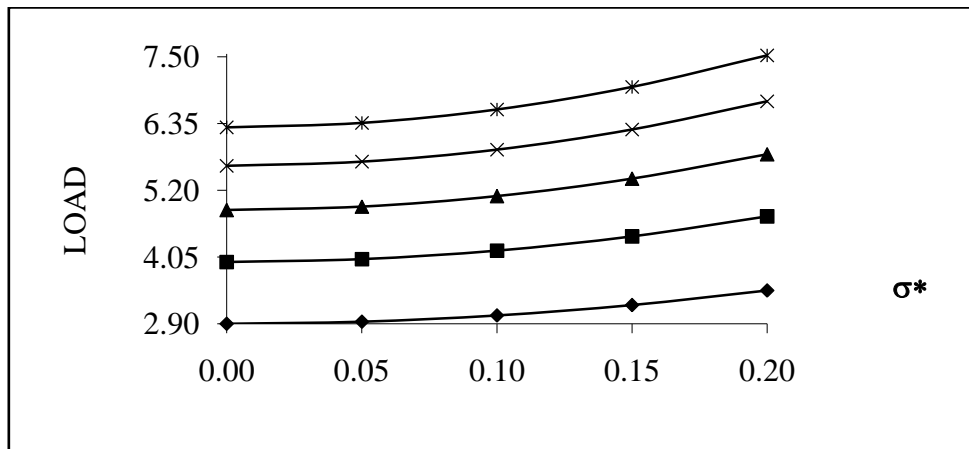


Figure: 17 load of σ^* & \square

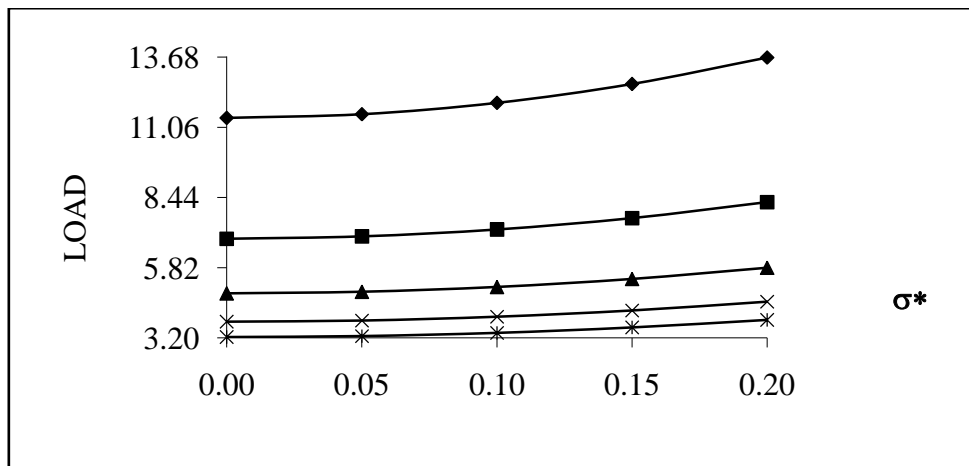


Figure: 18 load of σ^* & s*

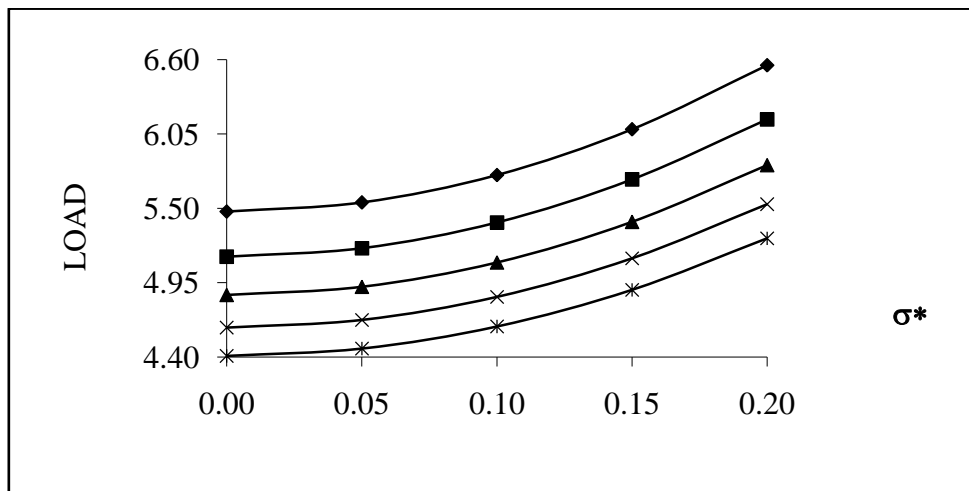


Figure: 19 load of α^* & ϵ^*

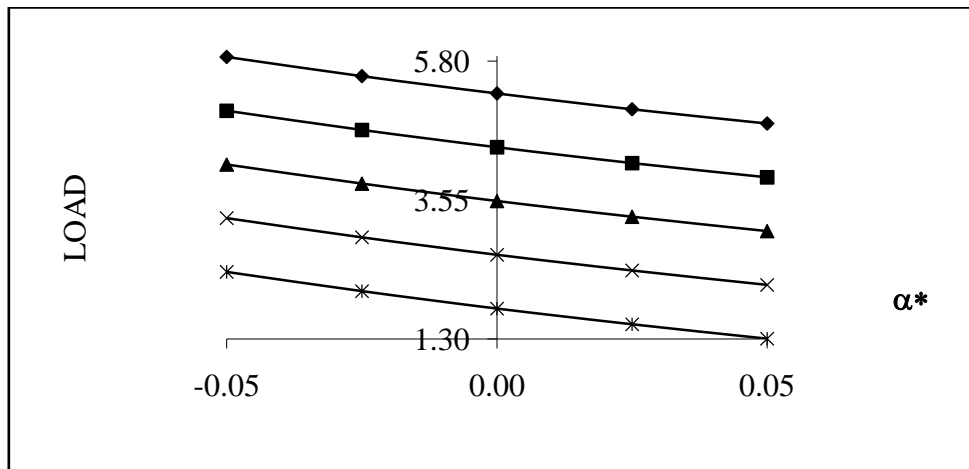


Figure: 20 load of α^* & k

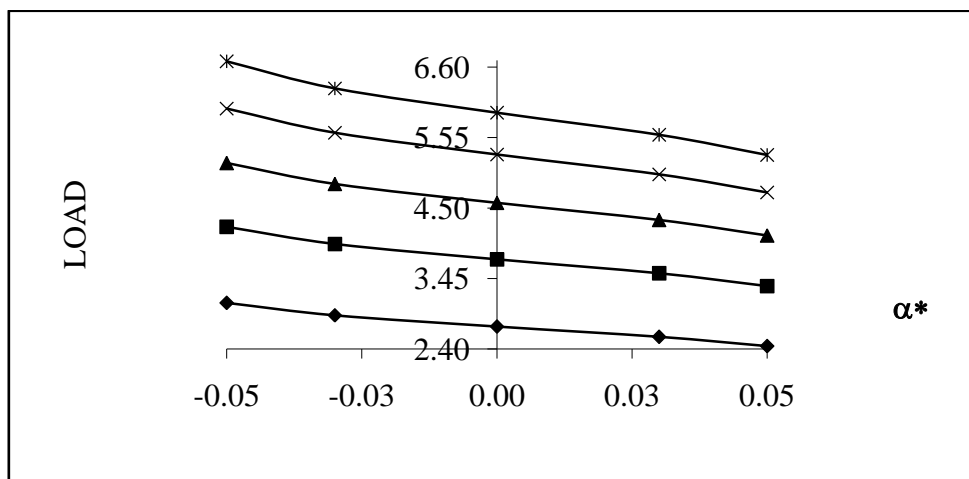


Figure: 21 load of α^* & \square

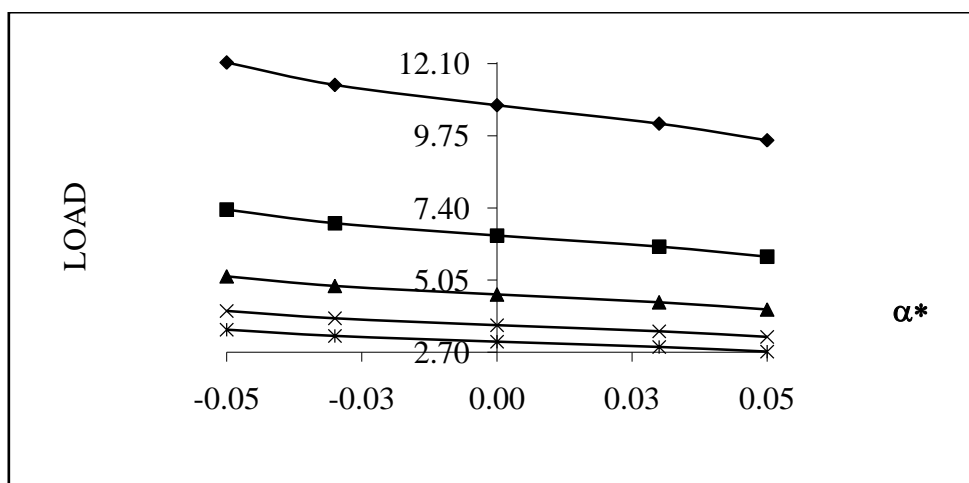


Figure: 22 load of α^* & s^*

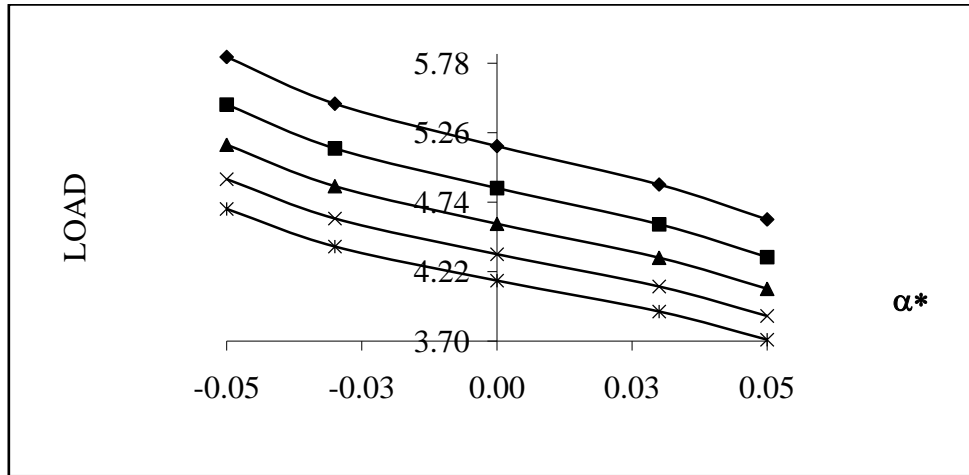


Figure: 23 load of ϵ^* & k

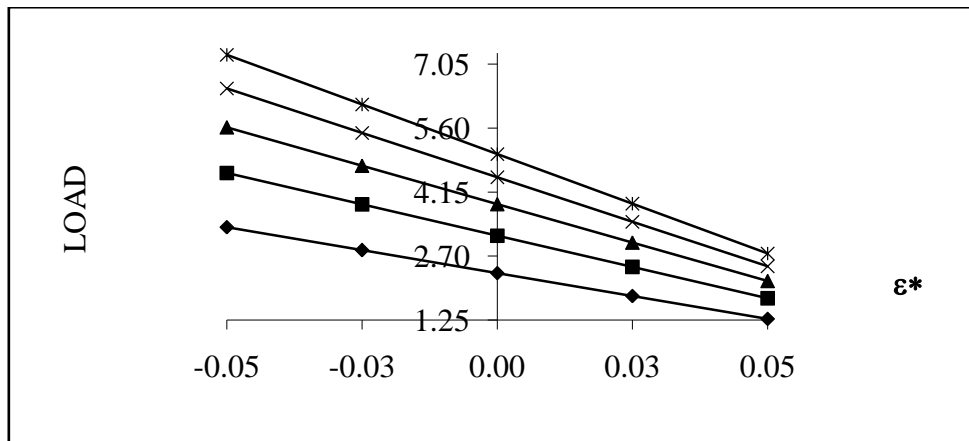


Figure: 24 load of ϵ^* & \square

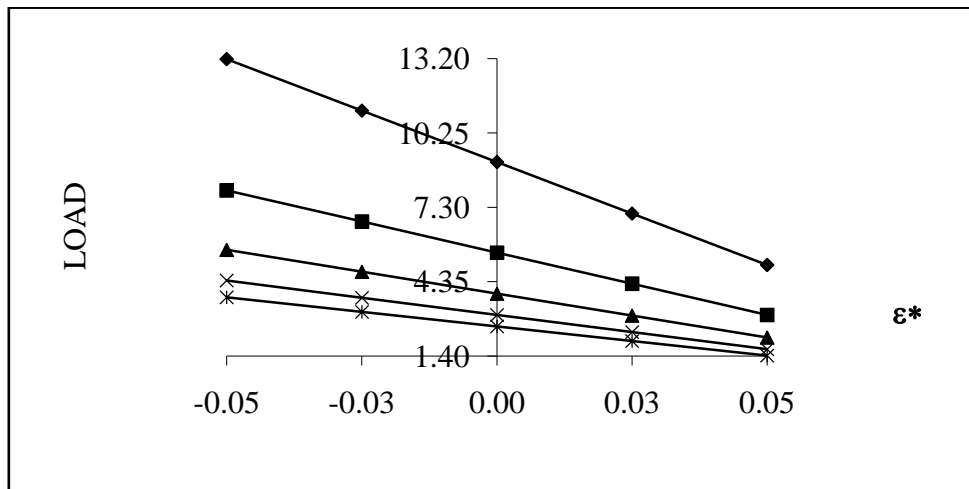


Figure: 25 load of ϵ^* & s^*

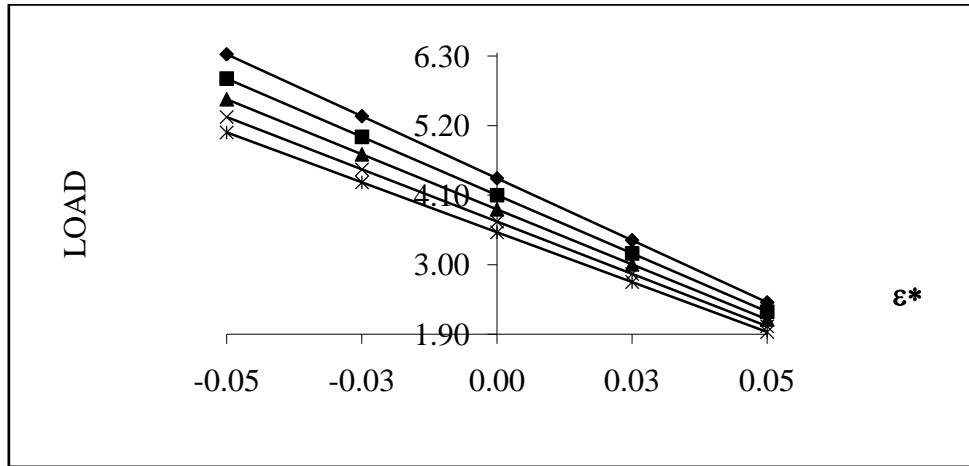


Figure: 26 load of k & \square \square

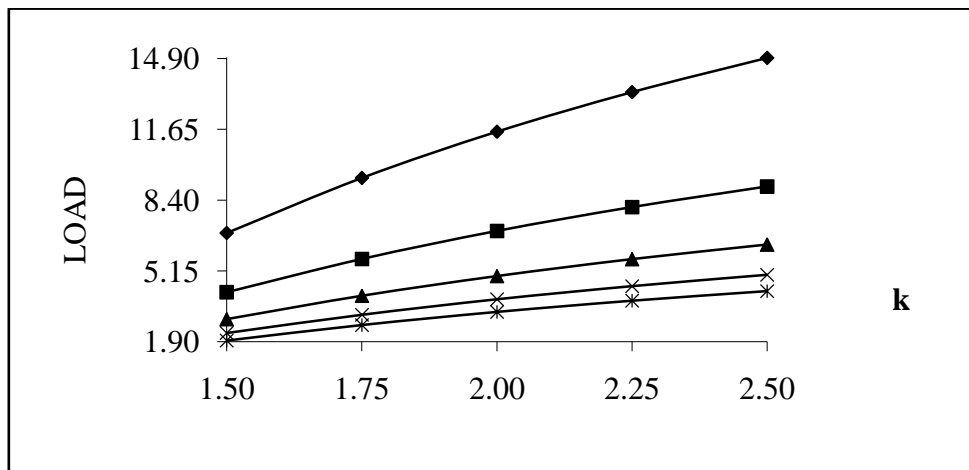


Figure: 27 load of k & s^*

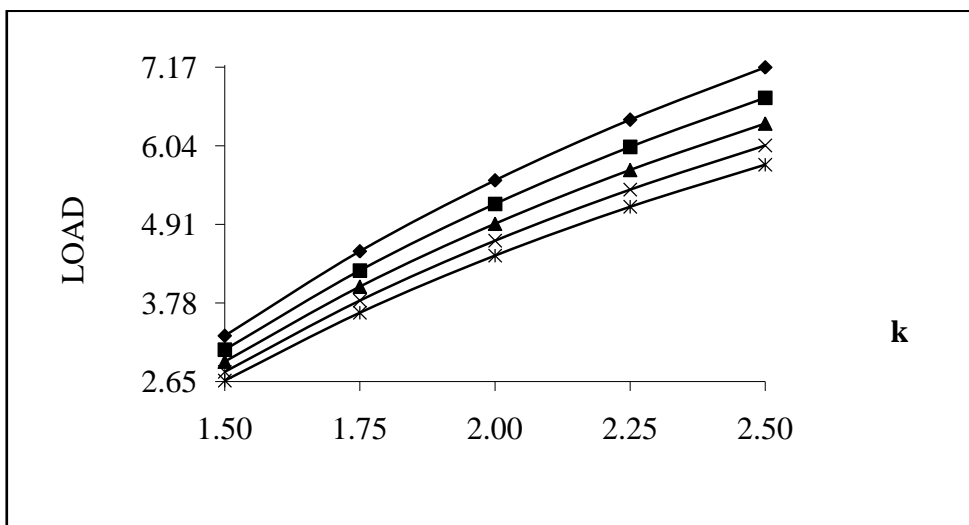


Figure: 28 load of \square & s^*

